

Study on the Variational Assimilation Technique for the Retrieval of Wind Fields from Doppler Radar Data*

WAN Qilin¹ (万齐林), XUE Jishan² (薛纪善), and ZHUANG Shiyu²(庄世宇)

1 Institute of Tropical and Marine Meteorology, CMA, Guangzhou 510080

2 Chinese Academy of Meteorological Sciences, Beijing 100081

(Received December 26, 2005)

ABSTRACT

This paper introduces a variational assimilation technique for the retrieval of wind fields from Doppler radar data. The assimilated information included both the radial velocity (RV) and the movement of radar echo. In this assimilation technique, the key is transforming the movement of radar echo to a new radar measuring variable—“apparent velocity”(AV). Thus, the information of wind is added, and the indeterminacy of recovering two-dimensional wind only by AV was overcome effectively by combining RV with AV. By means of CMA GRAPES-3Dvar and CINRAD data, some experiments were performed. The results show that the method of retrieval of wind fields is useful in obtaining the construction of the weather system.

Key words: variational assimilation technique, wind fields, Doppler radar data

1. Introduction

With widespread application of Doppler weather radar in the monitoring of mesoscale weather systems, information of the wind field observed by Doppler weather radars (abbreviated to the Doppler) has been received increasing attention. Retrieval of atmospheric wind field from Doppler observations has evolved from a hot research topic to a series of techniques.

Included in the first kind of technique are some retrieved wind fields that have been restrained with assumptions. As the Doppler can only measure the radial component of the wind vector relative to the radar, uncertainties exist in the wind field determined singly by the radial wind. By setting simple assumptions and restraints, the technique transforms uncertainties to certainties to derive mesoscale wind fields.

VVP (Volumn Velocity Processing) is one of the methods (Waldteufel and Corbin, 1979; Koscielny et al., 1982). Fitting the linear wind field with the least square method, it generally does not satisfy the requirements of mesoscale analysis (Koscielny et al., 1982). Following the mathematical relationship between the wind vector and radial vector, other approaches compute with some assumptions. The

first of them is VAP (Volume Azimuth Processing) (Tao, 1992; Lhermitte and Atlas, 1961; Browning and Wexler, 1968), which is, with the assumption that the wind vectors equal between any two points in contiguous direction angles on the same distance circle, a retrieval technique that is sensitive to changes in the radial wind to result in relatively large errors. The second is VAD (Velocity Azimuth Display), which assumes that the wind field varies homogeneously or linearly. The method was quite popular before and a number of improved schemes have been developed based on it (Scialom and Lemaitre, 1990; Shapiro et al., 1995; Jiang and Ge, 1997; Liu and Liu, 2000; Ma et al., 2000; Lang et al., 2001). For instance, the MAN-DOP by Scialom and Lemaitre (1990) is applicable for precipitation areas by both convective and stratiform clouds, GBVTD by Ma et al. (2000) is useful for vortex systems, etc. Highly depending on assumptions, all of these methods are limited in applicability and some of the assumptions are difficult to use in practice.

The second kind of technique involves some methods of variation and assimilation that combine with governing atmospheric equations. They are the same in essence with the 4-D variation and assimilation

*Supported by Research on Innovative Meteorological NWP Techniques in China (2001BA607B) and Research on Monitoring and Forecasting Techniques of Landfall Typhoon in China (2001DIA20026).

approaches of atmospheric data. Among them there is the simple adjoint function method (Qiu and Xu, 1992, 1996; Xu et al., 1994a,b; Laroche and Zawadzki, 1994; Xu and Qiu, 1995; Qiu et al., 2000), which turns problems into issues of parameter estimation by retrieving low-level mean velocity fields in a temporally averaged field radar-scanned for a number of times, based on reflectivity and/or radial velocity conservation equations and its adjoint equations. For areas where there is lack of radar measurement, difficulty occurs with governing equations and their adjoint ones and the interpolation in places distant from radar scanning (Qiu et al., 2000). Some representative work is the study on 3-D wind and thermodynamic fields as retrieved with singular Doppler data using the 4D-VAR technique based on cloud models (Sun et al., 1991; Sun, 1994; Sun and Crook, 1994). On its basis, the VDRAS system is built by NCAR. Specifically, Sun and Crook (1997) developed a warm-cloud model of VDRAS, and Wu et al. (2000) developed a mixed-phase model of VDRAS. Afterwards, Sun and Crook (2001) developed an operational system that could be used in the analysis and application of mesoscale synoptics. It is noted, however, all of these techniques have used models (or equations) that are independently designed and differ from the NWP system now in place for routine run. Greatly relying on the simplification of the governing equation sets for the atmosphere, they cannot be put into routine NWP operation as they are now. With the perfection of dynamic models, this kind of method will be useful.

Apart from the above work, the moving property of radar echoes is used to locate relevant cloud clusters to derive the wind field (Smythe and Zrnich, 1983; Tuttle and Foot, 1990; Tuttle and Gall, 1999), which is low in accuracy in meso- and micro-scale systems. A number of techniques and procedures have also been developed both at home and abroad that use dual Doppler data to retrieve wind fields, thermodynamic variables, and microphysical parameters of clouds. In view of the deployment strategy for the next-generation of weather radar in China (as in most other countries) that usually do not meet the needs of a dual-radar algorithm in terms of the distance be-

tween radars, they are not realistic to use with the current operational condition in China. No more cases will be introduced of retrieving with dual Doppler.

The prediction skill of a mesoscale NWP system depends much on whether the Doppler information is efficiently used. In NWP systems that use the above techniques to acquire atmospheric wind fields, there is failure of working integration between the techniques and existing assimilation and analysis systems (like those of widely used 3-D and new-developing 4-D), making the radar observation and data from other types of equipment two independent processes. In other words, information from other sources of observation cannot be used to improve the radar-retrieved wind field. Here, a technical scheme is put forward that acquires the atmospheric wind field by incorporating into the system of variation and assimilation two special items of temporal and spatial variation of radial wind velocity and echoes of the Doppler, which are part of the wind-field observation. It combines the radar-retrieved wind field integrally with the formation of model initial values, which can be used in both synoptic analyses and numerical prediction. With radar observations for South China, our technique was experimentally studied by incorporating it into the 3-D variational and assimilating system of GRAPES-3Dvar (Zhang et al., 2004), developed by the Numerical Prediction Research Center of the Chinese Academy of Meteorological Sciences.

2. Brief description of technical scheme

2.1 3-D variation and assimilation of atmospheric observations

It is assumed that the atmospheric dynamic and thermodynamic feature can be denoted by the vector of state x and the observed atmospheric feature by the vector of observation y . The relationship between the two vectors y and x is expressed by

$$y = H(x), \quad (1)$$

where H is the operator of observation. In addition to the observation, specific background information about the atmosphere is also known, which is called

the background or guess fields. The assimilation of atmospheric observations is achieved by correcting the background field based on the observation to make the latter agree with some basic patterns of atmospheric variation. Mathematically, it can be summed up as the issue of seeking solution to the minimization of the functional as follows.

$$\mathbf{J}(x) = \frac{1}{2} \left[(x - x_b)^T \mathbf{B}^{-1} (x - x_b) + (y - y_o)^T \mathbf{O}^{-1} (y - y_o) \right], \quad (2)$$

where the subscript b is the background, y_o is the observation, y is the observation calculated from x based on Eq.(1), and \mathbf{B} and \mathbf{O} are the matrices of covariance of the background and observational errors, respectively. The superscript T and -1 are the transposition and inverse of the matrix, respectively. Equation (2) is the target function of 3-D variation and assimilation. Given the condition of observation, background field, and statistics of relevant errors, the target function is tuned towards a minimized vector of state, or the analyzed value required. The operator of observation represented by Eq.(1) can be general. y can have physical attributes different from x . In other words, they can be physical quantities of different types so long as they are connected explicitly. It is then known from the angle of 3-D variation and assimilation that the difference between radar and conventional data is only in the operator of observation, which will be discussed below for its use in assimilating radar data.

2.2 Observation operator of radar-derived wind field

With the information of Doppler-derived wind field that has been assimilated with the 3-D variational technique in acquiring analyzed atmospheric wind field, the relationship between the wind field and radar observations needs to be known. As what has been said in the introduction section, two types of information are used in this work, temporal and spatial variations of radial velocity and echo of radar. They will be discussed separately here. The three components of wind, u , v , and w , are part of the vector of state in Eq.(1).

The relationship between the radial wind velocity

and wind vector is expressed by

$$S(V_R) = \frac{x - x_c}{R} u + \frac{y - y_c}{R} v + \frac{z - z_c}{R} (w - w_d), \quad (3)$$

where V_R is the observed radial wind velocity by radar, R is the distance from an observation point (x, y, z) to the site of radar (x_c, y_c, z_c) , u and v are two components of the horizontally analyzed wind field, w and w_d are the vertical velocity of air and the terminal velocity of cloud droplets, and S is the selected operator for the representation of the observation. According to scale analysis, the characteristic value of horizontal wind in synoptic systems is 1000 times as much as that of vertical wind and the characteristic value of horizontal wind in mesoscale systems is 100 times as much as that of vertical wind. The characteristic value of terminal velocity of cloud droplets is comparable to or a little larger than that of meso- and micro-scale systems. In view of the relatively small elevation angle of radar detection (the maximum is 19.5° with the latest generation of weather radar WSR-88D in China), the contribution of vertical velocity to the radial wind can be ignored. Only the horizontal wind field is studied here. Projecting Eq.(3) onto the horizontal plane, the third term disappears.

Setting

$$R_x = \frac{x - x_c}{R}, R_y = \frac{y - y_c}{R}, V_{sR} = S(V_R),$$

the relationship between the wind field analyzed with the variational and assimilation technique and the radar observations as expressed in Eq.(3) is transformed to

$$V_{sR} = R_x u + R_y v. \quad (4)$$

On the other hand, continuous changes in the intensity of radar echo can reveal the movement of cloud clusters with wind. For relatively short spans of time, especially, the echo intensity of clouds can be assumed to be in conservation, following Qiu et al. (1992, 1996, 2000), Xu et al.(1994 a,b, 1995), and Laroche and Zawadzki (1994), when local changes of the echo intensity are attributed to cloud advection. Meantime, the results of scale analysis indicate that the characteristic quantity of horizontal velocity in meso- and micro-scale systems is 100 times as much as that of

the vertical velocity while the characteristics of horizontal spatial scale are comparable to those of vertical one (for micro-scale) or one order of magnitude larger (for mesoscale). Following the estimation, the characteristic values of the vertical advection term for the echo intensity is at least one order of magnitude smaller than the horizontal advection term. Then, for mesoscale assimilation, the following simplified conservation equation of echo intensity is based to locate and study the other relation between the wind field and radar observation. The equation can be written as

$$\frac{\partial S(I)}{\partial t} = -\frac{\partial S(I)}{\partial x}u - \frac{\partial S(I)}{\partial y}v, \quad (5)$$

where I is the intensity of radar echo, S is the selected operator for the representation of the observation and other symbols follow conventional meteorological meanings.

Equation (5) can indicate the dimension of wind speed. For this purpose, we introduce the following

$$\begin{aligned} I_{sD} &= \sqrt{\left(\frac{\partial S(I)}{\partial x}\right)^2 + \left(\frac{\partial S(I)}{\partial y}\right)^2}, \\ I_{sx} &= -\frac{\partial S(I)}{\partial x} / I_{sD}, \quad I_{sy} = -\frac{\partial S(I)}{\partial y} / I_{sD}, \\ V_{st} &= -\frac{\partial S(I)}{\partial t} / I_{sD}. \end{aligned}$$

Then, we have

$$V_{st} = I_{sx}u + I_{sy}v, \quad (6)$$

where V_{st} is the quantity reflecting the temporal and spatial variations of echo, which equals the component of wind field in the direction of gradient vector, indicating the velocity of echo movement with wind. If the gradient at a given point is vertical to the wind vector, no movement of echo will be evident there and V_{st} equals zero. If the gradient is parallel to the wind vector, the echo can be seen moving at wind velocity and V_{st} equals the wind speed. Here, V_{st} , the new ‘‘measured quantity of radar’’, is called the ‘‘apparent wind velocity’’ of radar. It is evident that the apparent wind velocity has definite physical meaning, which helps determine observational errors and control the quality of data.

Compared with the direct use of Eq.(5), advantages are obvious in employing the relation between the analyzed wind field and radar observation as expressed in Eq.(6) for reasons listed below. For areas where there is significant spatial change in echo intensity (where the given threshold value for horizontal gradient is satisfied), the local change in echo intensity within the short duration is contributed by advection more than cloud clusters; the ‘‘apparent wind velocity’’ exists and accurately depicts the wind field, which is then incorporated into the assimilation system. For areas where there is insignificant spatial change in echo intensity, the local change in echo intensity is contributed more by cloud clusters but does not reflect the information about the wind field. No ‘‘apparent wind velocity’’ can be calculated using Eq.(6), which is treated as lack of observation. It automatically prevents data incapable of describing the wind field from being included into the assimilation system. In contrast, the application of Eq.(5) does not rid the system from the effects of cloud clusters as it does not filters out inadequate data as Eq.(6).

In our work, the operator S follows the Barnes interpolation-filter scheme for radar measurements at different time and location to obtain grid point values for a given time and spatial resolution. Meantime, it is also necessary to run selective filtering for representative scales. The weighting function for interpolation-filter is given by

$$W(\Delta x, \Delta y, \Delta z, \Delta t, \alpha, \beta, \gamma) = e^{-4\left(\frac{\Delta x^2 + \Delta y^2}{\alpha^2} + \frac{\Delta z^2}{\beta^2} + \frac{\Delta t^2}{\gamma^2}\right)}, \quad (7)$$

where $\Delta x, \Delta y, \Delta z$, and Δt are the spatial distance and temporal deviations from designated gridpoints, respectively, α, β , and γ are selection parameters of horizontal, vertical, and temporal scales, respectively.

The scheme of variation and assimilation with the radar wind-field data put forward in this work takes V_{sR} , the radial wind velocity, and V_{st} , the ‘‘apparent wind velocity’’ as the observed quantity to determine the atmospheric wind field using the variational and assimilation technique. Then, from Eqs.(4) and (6), the vectors of transformation operators for the two

observed quantities are respectively

$$\mathbf{R} = \begin{bmatrix} R_x \\ R_y \end{bmatrix}, \quad (8)$$

$$\mathbf{I}_s = \begin{bmatrix} I_{sx} \\ I_{sy} \end{bmatrix}. \quad (9)$$

It is found that \mathbf{R} is the radial unit vector of radar and \mathbf{I}_s is the unit vector of echo intensity (which has been selected for representation) in the horizontal gradient.

It is easy to calculate the measurements—radial wind velocity V_{sR} and “apparent wind velocity” V_{st} . In practice, however, quality control must be run of the two radar measurements to delete unreasonable, abnormal values. The following conditions must be met for the selected point of measurement:

(1) For radial wind velocity V_{sR} , $R \geq R_0$ is selected (with 0.01 long./lat.);

(2) For the “apparent wind velocity” V_{st} , $|V_{st}| \leq V_{tm}$ must be met (by taking 50.0 m s^{-1}). At the same time, the horizontal gradient for corresponding echo intensity must satisfy $I_{do}(= 0.0001 \text{ dBz m}^{-1}) \leq I_{sD} \leq I_{dm}(=0.005 \text{ dBz m}^{-1})$. It must be noted that the thresholds given here are for cases in which the volume scan is 6 min with the horizontal gridpoint interval at 2 km in data processing (of selection for representation). The threshold is suggested to be adjusted for cases other than it.

(3) For measurement points with radial wind velocity, the “apparent wind” is deleted if the included angle between its direction and the radial direction of radar is less than 15° .

From Eqs.(4) and (6), it is seen that the selected V_{sR} and V_{st} show linear relationship with the assimilated wind field. Thus, the corresponding adjoint operator is the transposition matrix for Eqs.(8) and (9).

In carrying out 3-D variation and assimilation,

errors of the observation must be specified, usually at $1-3 \text{ m s}^{-1}$ for V_{sR} and $1-5 \text{ m s}^{-1}$ for V_{st} , respectively.

3. Experiments and analyses

The current work uses the 3-D variational and assimilating system of GRAPES-3Dvar as research basis, which has been proved in some experiments to have good capabilities. Here, relevant observational operators and adjoint operator procedures are added to the system following the scheme described in the previous section to construct a 3-D variational system that is able to assimilate wind field data measured by Doppler weather radars.

During the analysis, the characteristics and errors are studied on a contour chart. The technique is also applicable for three dimensions.

The data used are all from the “Research on the Monitoring and Forecasting Technique for Disasters by Landing Typhoons in China” (2001DIA20026), a key public-welfare project of the Ministry of Science and Technology. Radar data taken in Hongkong are used to study the technical scheme, owing to their wide coverage and high-quality CAPPI data (including echo intensity and radial wind velocity).

3.1 Single-point experiment

To understand the role and characteristics of V_{sR} and V_{st} in the variation and assimilation, a single point (24.35°N , 114.40°E , 3 km in height, which is equivalent to 700 hPa) is selected near the sounding station (59096) for the experiment. The zonal wind is -13.1 m s^{-1} , meridional wind -9.2 m s^{-1} , and Table 1 gives the relevant radial wind velocity and “apparent wind velocity” measurements (which are selected for representation).

Figure 1 gives the analyzed wind field with the single-point data without the background stream (the same below). Figure 1a is the wind field achieved by

Table 1. Radial wind velocity and “apparent wind velocity” at 02080205UTC (denoted as 0500 UTC, August 2, 2002, the same below; m s^{-1})

	Observations (m s^{-1})	Transformation operators <i>x</i> component	Transformation operators <i>y</i> component	Errors (m s^{-1})
Radial wind velocity	-8.76	0.068	0.998	1.0
Apparent wind velocity	-2.96	0.849	-0.528	1.0

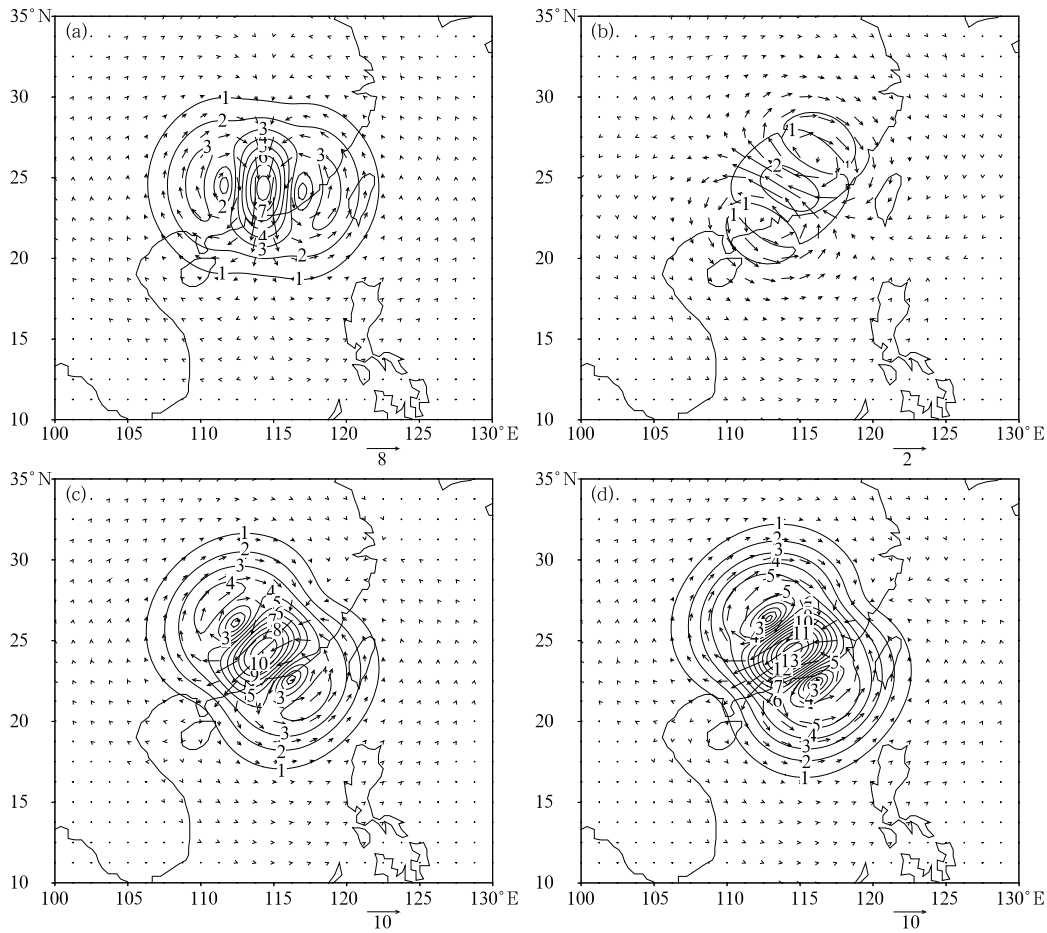


Fig.1. The analyzed wind fields with the data at single point in the case of no background stream. (a) Radial velocity assimilated, (b) “apparent velocity” assimilated, (c) both radial velocity and “apparent velocity” assimilated, and (d) radiosounding data assimilated.

assimilating the radial wind velocity, Fig.1b the wind field obtained by assimilating the “apparent wind velocity”, Fig.1c the wind field by jointly assimilating the above two types of information, and Fig.1d the wind field by analyzing the radiosounding data. The figures show that 2-D wind vector is determined by just one observed variable whether the assimilation concerns with radial or “apparent” wind velocity and the wind vector is not accurate due to the effect of uncertainty. They also reveal a common feature that the two cases both have wind vectors with the same direction as the transformation vector. It shows that neither the radial nor “apparent” wind velocity can secure the availability of wind fields that agree with reality. If, however, the radial and “apparent” wind

fields are jointly assimilated, the wind field so determined will be consistent with the one obtained with radio sounding data. It indicates that the “apparent wind velocity” is an extra source of wind field observation that plays an important role in the determination of atmospheric wind fields.

3.2 Multiple-point experiment

If the radial and “apparent” wind velocities measured by radar at all spatial points are incorporated into the variation and assimilation system, what will come out of it with variational restraints?

The observations for tropical cyclone “Kammuri” as measured by the Hongkong radar at 02080500 UTC were used. For the time, the center of the storm was

at 23°N, 115°E, and had intense vortex structure for it just made landfall.

Figure 2 gives the radial wind velocity by radar at the altitude of 3 km. Specifically, Fig.2a is the radial velocity that has been through selection for representation, and Figs.2b and 2c are two components of the transformation operator for the quantity. The figures show that the data are quite complete and clearly describes the radial component of the tropical cyclone circulation. Meanwhile, the operator shows radiative state. As the storm is to the east of the radar and within the center of the vortex, the x component has larger share so that the radar detects strong radial wind velocity and large radial wind shear.

Figure 3 gives the echo of radar intensity and “apparent wind velocity”. Specifically, Fig.3a is the radial velocity that has been through selection for representation, and Figs.3b and 3c are two components of the transformation operator for the quantity. The figures show that the data are quite complete and

clearly describes the radial component of the tropical cyclone circulation; corresponding radar “apparent wind velocity” and the two components of the associated transformation operator distributed over most of the area covered by the echo. Some points of the “apparent wind velocity” are blank, resulting from screening for quality control. The blank points are actually those with small gradient of echo and the contribution from wind advection cannot be isolated from that from cloud clusters. They are thus deleted. The “apparent wind velocity” retained suggests that the points’ gradient of echo is so large that echo changes can be viewed as the consequence of wind advection for short intervals of time, which is just what wind field analysis needs. In addition, the blank points do not bring difficulty to processing, as the data, in the form of random points of measurement, are incorporated into the 3-D variational system, which is restrained by some physical and mathematical relation.

Figure 4 gives the analyzed wind field with

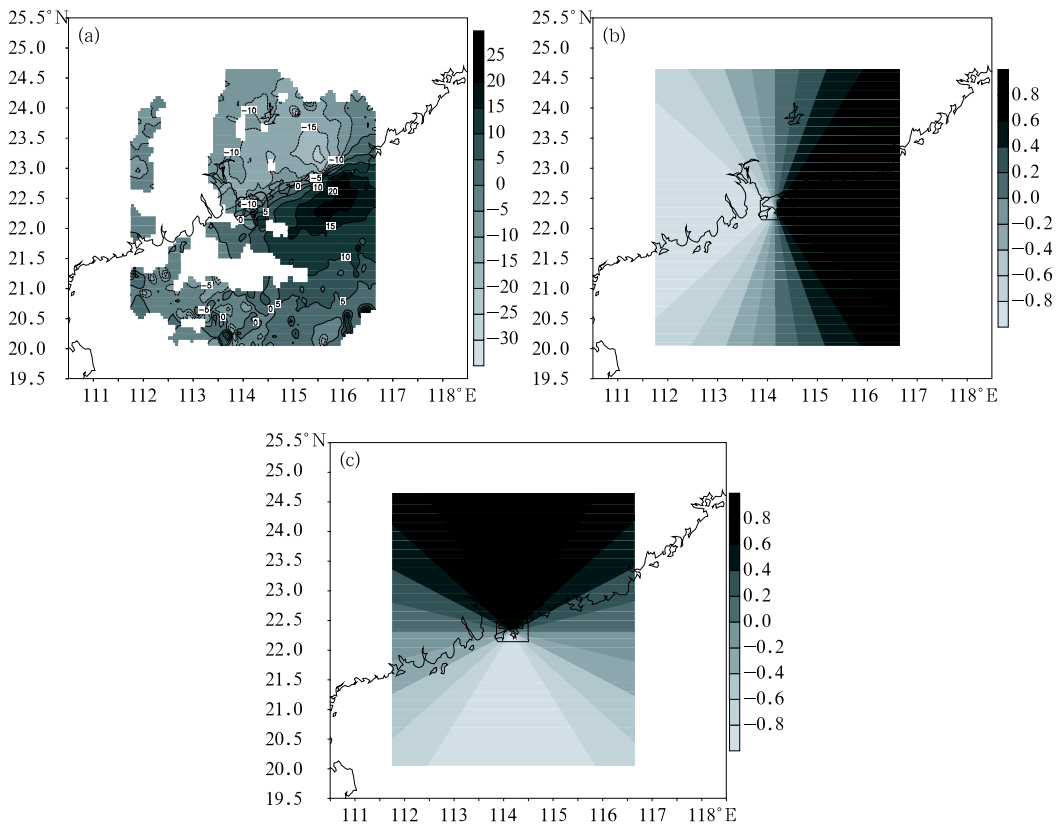


Fig.2. Data of radial velocity. (a) Radial velocity (m s^{-1} , the same below), (b) x -component of observation operator, and (c) y -component of observation operator.

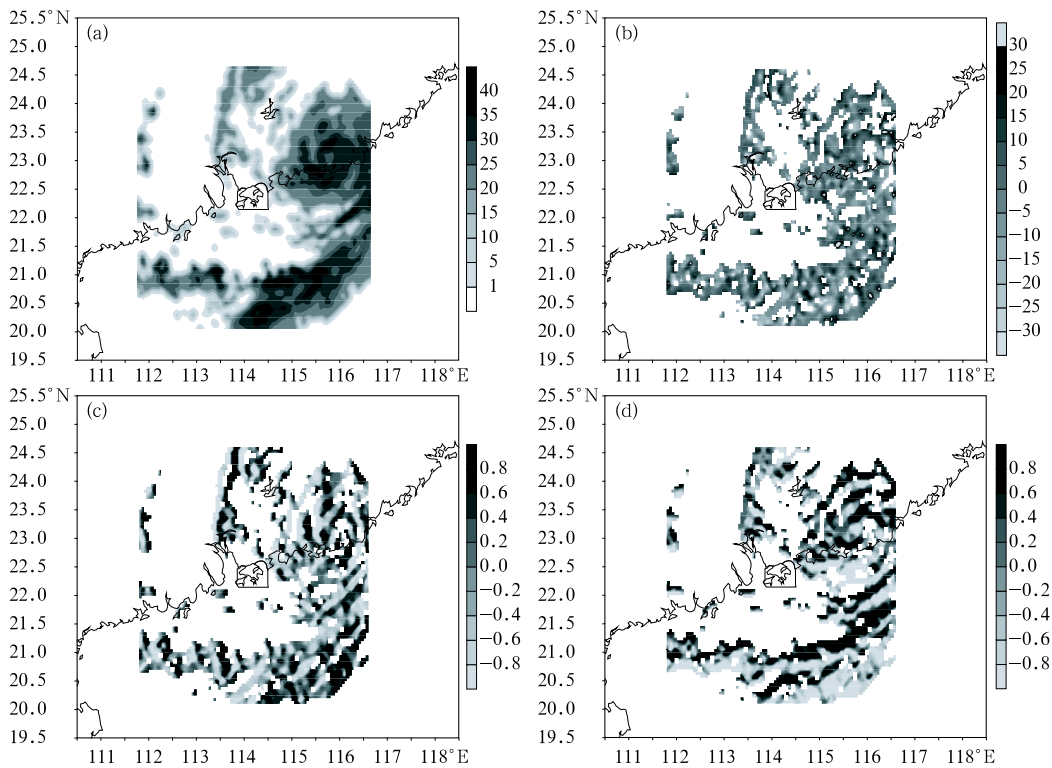


Fig.3. Processing of radar echo intensity. (a) Echo intensity after selection of representation (dBz), (b) “apparent velocity” (m s^{-1}), (c) x -component of observation operator, and (d) y -component of observation operators.

multi-point variation and assimilation without the background stream. Figure 4a is the wind field achieved by assimilating the radial wind velocity, Fig.4b the wind field obtained by assimilating the “apparent wind velocity”, Fig.4c the wind field by jointly assimilating the above two types of information, and Fig.4d the wind field by analyzing the radiosounding data. It shows that vortex circulation can be obtained for the tropical cyclone with the control of variational restrains, whether the radial or “apparent” wind velocity is assimilated. If, however, the radial wind velocity is assimilated, the location of vortex center is deviated from the observation and the azimuth is not reasonable for the high-wind area; if the “apparent wind velocity” is assimilated, the location of vortex center and distribution of high-wind are quite reasonable but the vortex intensity is much weaker. Only with joint assimilation of the radial and “apparent” wind velocity can the location of vortex center, distribution of high-wind areas, and vortex intensity be more reasonable

than the previous two choices. Besides, the shape of vortex circulation obtained with radio sounding data is less realistic, which is associated with the scarcity of radio sounding data.

Figure 5 gives the radial component retrieved with the scheme in relation to the radar without the background stream using multi-point data. The figure reveals the following findings. With the radial wind velocity (Figs.5a and 5c) assimilated, the radial component of the obtained wind field is consistent with that measured by radar. Assimilating the “apparent wind velocity” (Fig.5b) will only obtain a much smaller radial component. Analyzing with the sounding data will result in a horizontal distribution of radial component in large discrepancy with radar measurement.

From the statistical analysis of errors for the wind field determined with the scheme without the background stream using multi-point data (Table 2), the mean square deviation and relative error can be smaller than any other choices if the radial wind

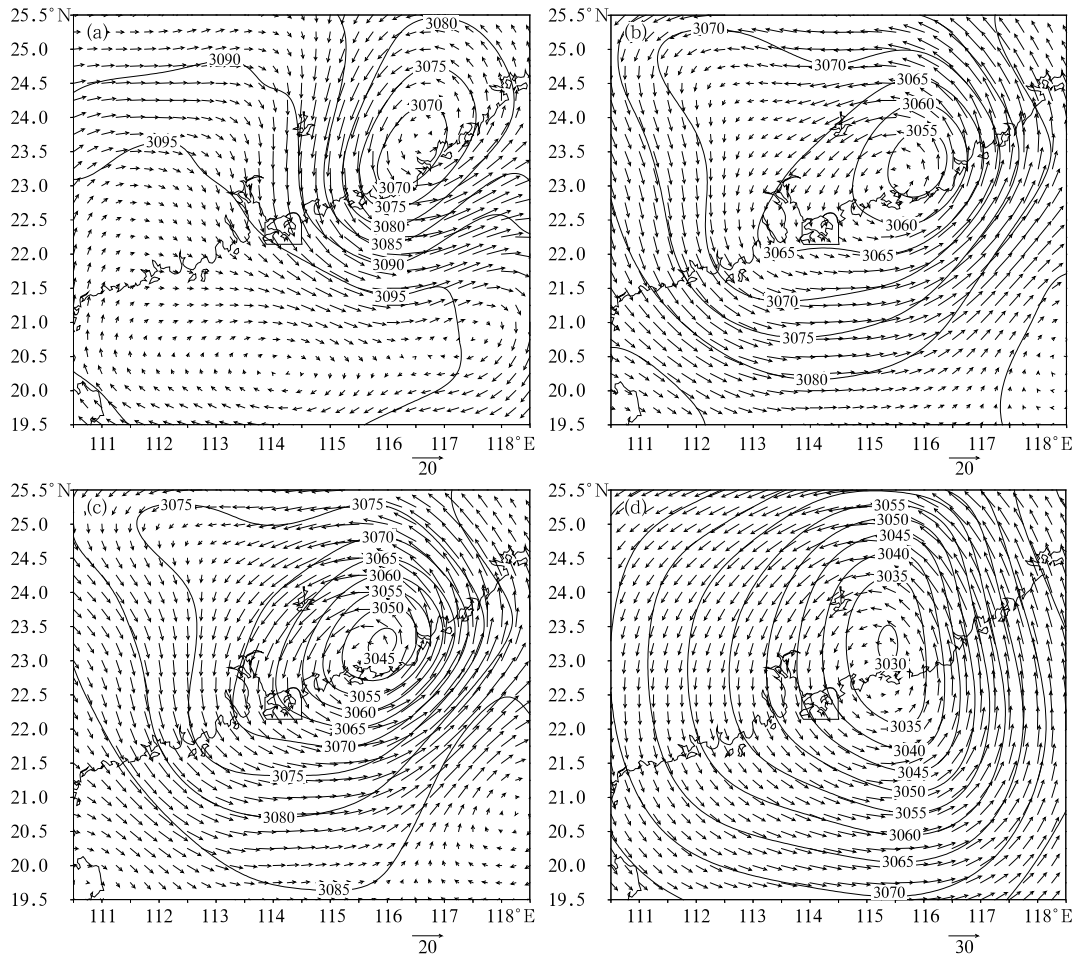


Fig.4. The analyzed wind fields with no background stream. (a) Radial velocity assimilated, (b) “apparent velocity” assimilated, (c) both radial velocity and “apparent velocity” assimilated, and (d) radiosounding data assimilated.

velocity is assimilated or the error can be much larger; only with both the radial and “apparent” wind velocities assimilated, can the mean square deviation and relative error be smaller than any other choices; with only the radial wind velocity assimilated, the error is the largest for wind field versus radio sounding; the error of radial component is the largest for wind field

versus radar if the wind field is analyzed with radio sounding data.

In summary, joint assimilation of the radial and “apparent” wind velocities can yield good overall result of the wind field with the minimum error, which is also a scheme strongly recommended in this work. Meantime, in another experiment with the

Table 2. Statistic analysis of errors of wind field analyzed with the variational and assimilation scheme with multi-point data and absence of background stream

	Compared with radial wind velocity of radar (6384 points)		Compared with radiosounding wind (4 points)	
	RMS deviation (m s^{-1})	Relative error (m s^{-1})	RMS deviation (%)	Relative error (%)
Radial wind velocity of radar	3.9	39	10.7	73
“Apparent wind velocity” of echo	5.7	57	6.4	46
Radial and “apparent” wind velocity	4.0	39	3.1	21
Radiosounding wind	6.7	59	2.1	17

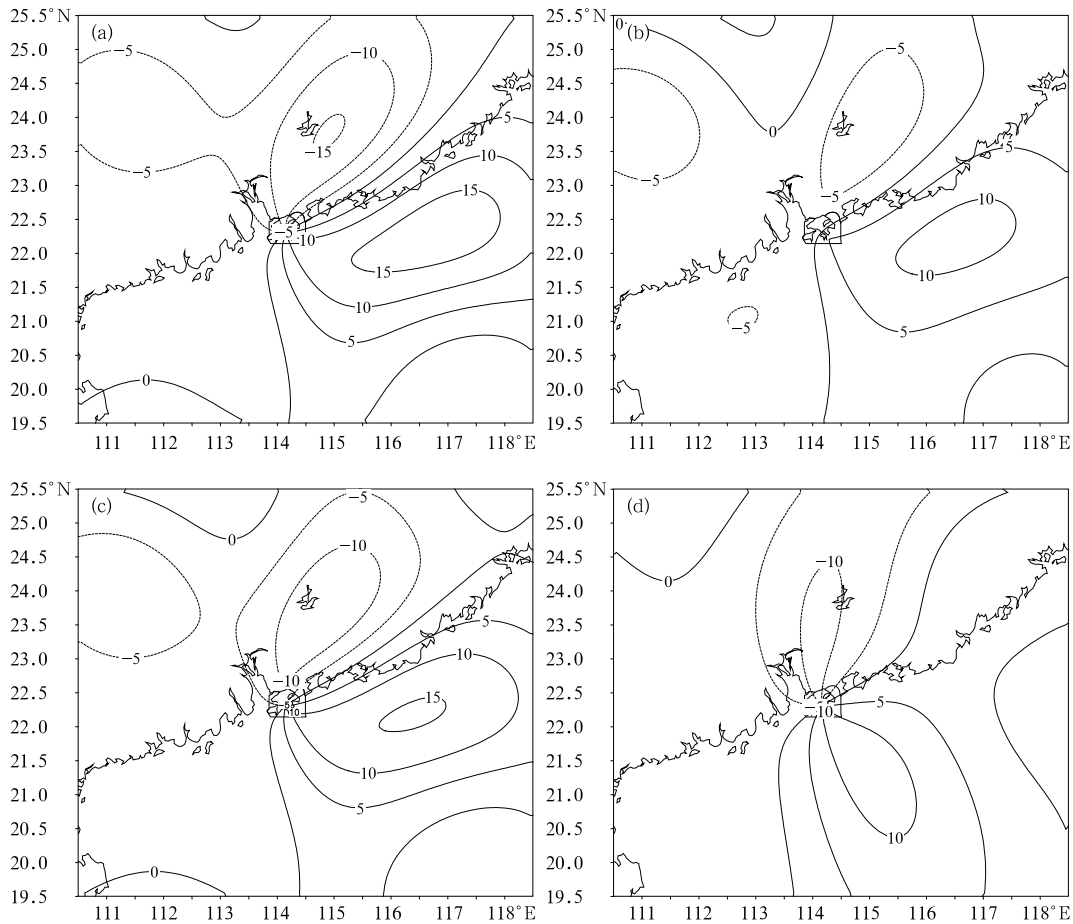


Fig.5. The radial component of analyzed wind field with no background stream. (a) Radial velocity assimilated, (b) “apparent velocity” assimilated, (c) both radial velocity and “apparent velocity” assimilated, and (d) radiosounding data assimilated.

background stream conducted by the authors, results in that completely resemble to those without the background stream are found (figure omitted). It shows that the scheme proposed in this work is comparable with the background stream. In addition, as the assimilation system is able to assimilate data of sounding, surface observation, and satellite remote sensing, the inclusion of radar data in this scheme does not have conflicts. The presence of all these types of data in the same assimilation system acts to supplement and restrain each other.

4. Real cases

To further verify the operational usefulness and applicability of the scheme, experiments will be done

with the following few cases. It should first be noted that the experiments use the data now in operational runs in the new generation of weather Doppler radar system in Guangdong Province, and data processing, which includes the selection for representation of measurements, processing and quality control of the radial and “apparent” wind velocities, etc., is conducted on the cones volume-scanned by radar.

The basic state of atmospheric circulation consists of vortex flows and straight flows (the troughs, ridges or shear lines can be seen as their transformations and combinations). Their real cases are used in the study. For the vortex flow, particularly, different locations have to be isolated from the vortex center relative to the radar.

4.1 Type one: vortex center in the neighborhood of radar and radial wind velocity without well-defined shear

Figure 6 gives the 3-km measurements at 02091118 UTC taken by a radar in Yangjiang city, Guangdong Province. Figure 6a gives the echo of radar intensity, and Fig.6b the radial wind velocity of radar after the selection for representation. It shows that both of them have complete datasets that clearly describe the spiral system of the tropical cyclone and the radial component of the tropical cyclone relative to the radar. In the vortex area, however, the field of radial wind velocity does not have significant information of wind shear and the entire field has characteristics similar to the radial component of southeasterly straight flow. No information of strong vortex circulation is available only from the radial wind velocity field of radar.

Figure 7 gives the wind field analyzed with variation and assimilation using the radar data in Yangjiang, Guangdong Province at 02091118 UTC. Figures 7a and 7b are the wind fields acquired by assimilating the radial wind velocity and the radial component relative to the radar. Figures 7c and 7d give the wind field obtained by assimilating the “apparent wind velocity”, and the radial component relative to the radar. Figures 7e and 7f present the wind field de-

termined by jointly assimilating the radial wind velocity and “apparent wind velocity”, and the radial component relative to the radar. The figures show that if only the radial wind is assimilated, the radial component of the wind field obtained is consistent with that measured by radar, but displays itself as quasi-straight southerly wind for the lack of vortex circulation of the tropical cyclone. It is obvious that no correct wind field is determined if the radial velocity of radar is assimilated. It fully reflects the uncertainty of 2-D wind vectors based on single measurements and shows that it is very necessary to include information about the wind field other than the radial wind velocity. If the “apparent wind velocity” is assimilated, vortex circulation for the tropical cyclone can be determined with 3-D variational restrains and realistic location of vortex center is obtained for the wind field, but with much smaller radial component. It shows that the shape of the wind field circulation is right but with large numerical deviation, unable to depict strong winds with the tropical cyclone. The location of vortex center and vortex intensity are more reasonable when the radial wind velocity and “apparent wind velocity” are jointly assimilated and its radial component is also close to that measured by radar.

Figure 8 gives the comparison between the meridional circulation of a wind field analyzed with radar data from Yangjiang, Guangdong Province (going

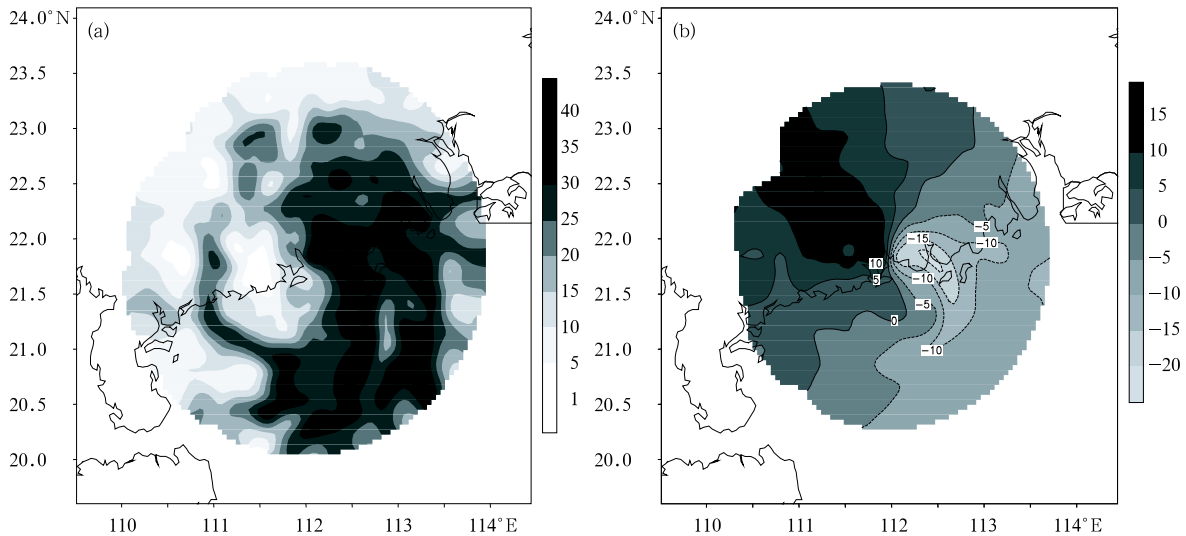


Fig.6. Radar data in Yangjiang, Guangdong Province, at the height of 3 km (02091118UTC). (a) Echo intensity, and (b) radial velocity (m s^{-1}).

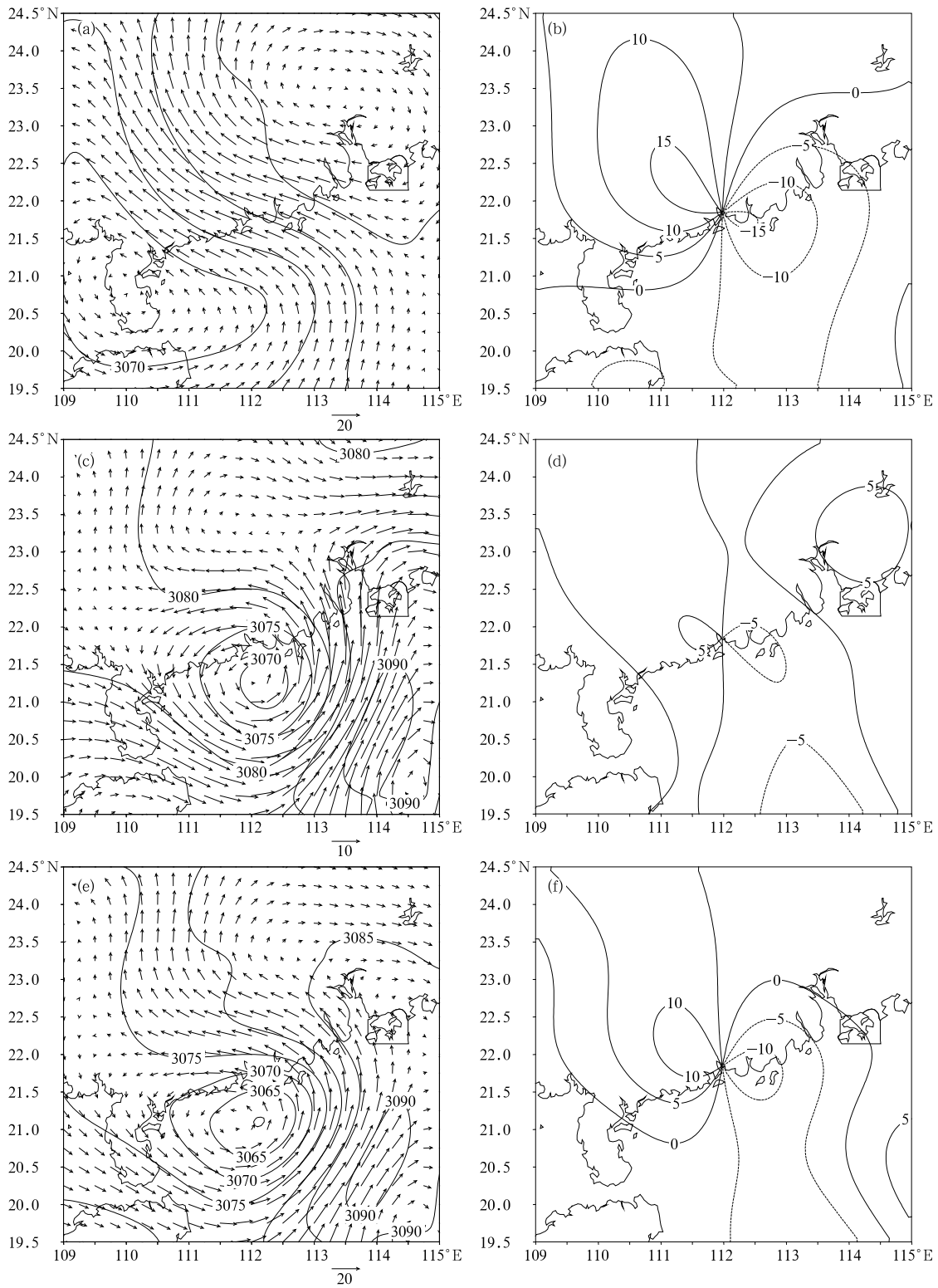


Fig.7. The analyzed wind fields with radar data in Yangjiang, Guangdong Province. (a) Radial velocity assimilated, (b) radial component corresponding to that in Fig.7a, (c) "apparent velocity" assimilated, (d) the radial component corresponding to that in Fig.7c, (e) both radial velocity and "apparent velocity" assimilated, and (f) radial component corresponding to that in Fig.7e.

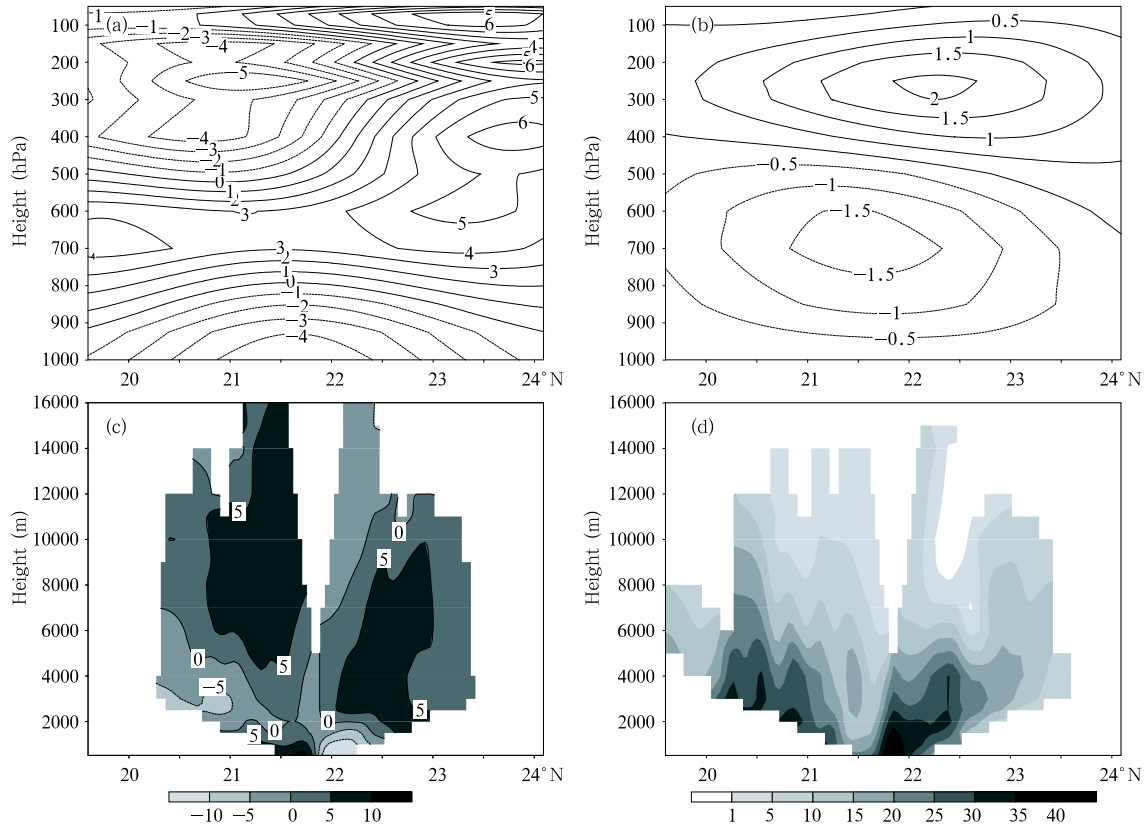


Fig.8. The vertical section along 112°E (passing through the radar). (a) The meridional component of analyzed wind (m s^{-1}), (b) vertical velocity ($\times 10^{-3} \text{ hPa s}^{-1}$), (c) radial velocity (m s^{-1}), and (d) radar echo intensity (dBz).

through the radar site on a vertical cross-section along 112°E with the radial wind velocity and “apparent wind velocity” jointly assimilated) and the radar measurements. Figure 8a is the meridional component obtained for the wind field, Fig.8b the vertical velocity of wind field, Fig.8c the radial wind velocity measured by radar, and Fig.8d the intensity of radar echo. The figures show that the meridional component obtained for the wind field corresponds well with the radial wind measured on the cross section, which agrees with the horizontal distribution. It shows from another angle that wind fields determined with the variational and assimilation scheme have reasonable 3-D structure. Meantime, judging from the vertical velocity (as diagnostically derived from the horizontal wind field and continuity equations), it is known that the wind field can depict the systematic updraft in the tropical cyclone and corresponds well with the

intensity of radar echo. The eye area is not picked up, which is linked with scale selection. In addition, the assimilated wind field is relatively poor in upper tropospheric levels (above 9 km), which is associated with the ways the radar works.

4.2 *Type two: vortex center some distance away from the radar and radial wind velocity with well-defined shear*

Figure 9 gives the 3-km measurements at 02080500 UTC taken by a radar in Meizhou city, Guangdong Province. Figure 9a gives the echo of radar intensity, and Fig.9b the radial wind velocity of radar, after the selection for representation. It shows that both of them have complete datasets that clearly describe the spiral system of the tropical cyclone and the radial component of the tropical cyclone relative to the radar. Particularly, there is obvious shear in

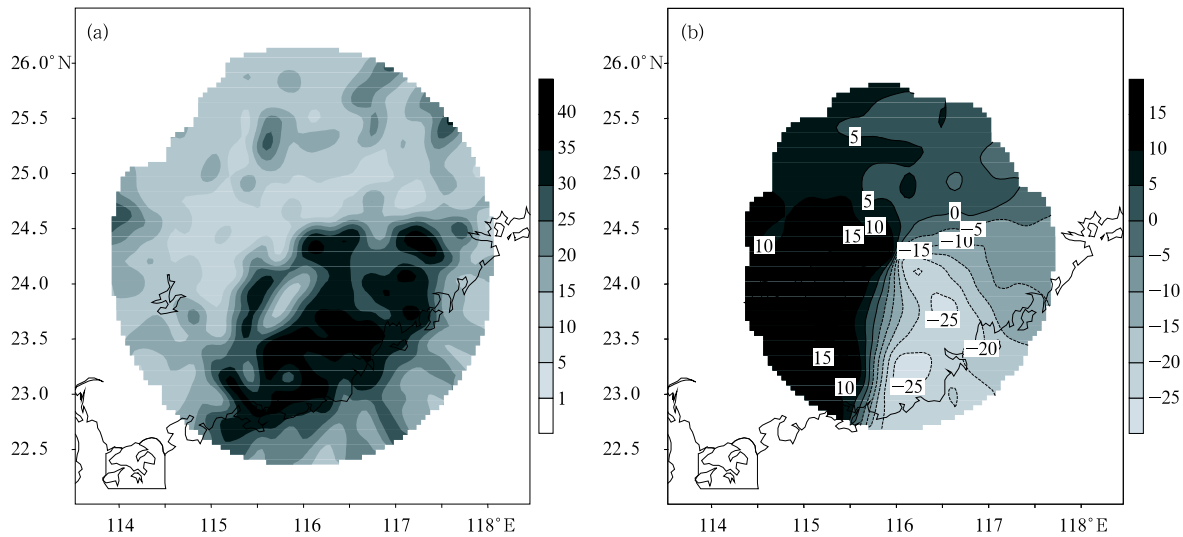


Fig.9. Radar data in Meizhou city, Guangdong Province at the height of 3 km (02080500UTC). (a) Radar echo intensity (dBz), and (b) radial velocity (m s^{-1}).

the vortex area of the radial velocity field.

Figure 10 gives the comparison between the meridional circulation of a wind field analyzed with radar data from Yangjiang, Guangdong Province (going through the radar site on a vertical cross-section along 112°E with the radial wind velocity and “apparent wind velocity” jointly assimilated) and the radar measurements. Figure 10a is the meridional component obtained for the wind field, Fig.10b the vertical velocity of wind field, Fig.10c the radial wind velocity measured by radar, and Fig.10d the intensity of radar echo. Figures 10e and 10f are the wind fields determined by jointly assimilating the radial and “apparent” wind velocity and the radial component relative to radar. The figures also show that the vortex circulation for the tropical cyclone can be determined with 3-D variational restrains, whether the radial or “apparent” wind velocity is assimilated. If the radial wind velocity is assimilated, the derived radial component of wind agrees with the radar-measured radial wind velocity but with more southward location of the vortex center. If only the “apparent wind velocity” is assimilated, the derived location of vortex center is more realistic but with loose and weak circulation in addition to much less realistic horizontal distribution and magnitude of the radial component. Only with joint

assimilation of both the radial and “apparent” wind velocity can we obtain reasonable location of vortex center and vortex intensity and consistent with the radial wind velocity measured by radar. In other words, joint assimilation of the two types of information gives the best result and adding the “apparent wind velocity” will benefit the acquisition of atmospheric wind fields through variation and assimilation.

Similar results are found in the analysis of other cases and will be omitted here.

4.3 Type three: straight basic airflow with mesoscale convection

Figure 11 gives the 3-km measurements at 03061012 UTC taken by a radar in Yangjiang, Guangdong Province. Figure 11a gives the echo of radar intensity, and Fig.11b the radial wind velocity of radar, after the selection for representation. The figures show complete data of radar echoes that clearly describe an arc-shaped convective cloud band running from north to south; the data of radial wind velocity are also quite complete, which describe the radial component of a southwesterly straight flow relative to the radar. At that time, a consistent southwesterly wind (at 700 hPa) was prevailing over the area of Guangdong Province.

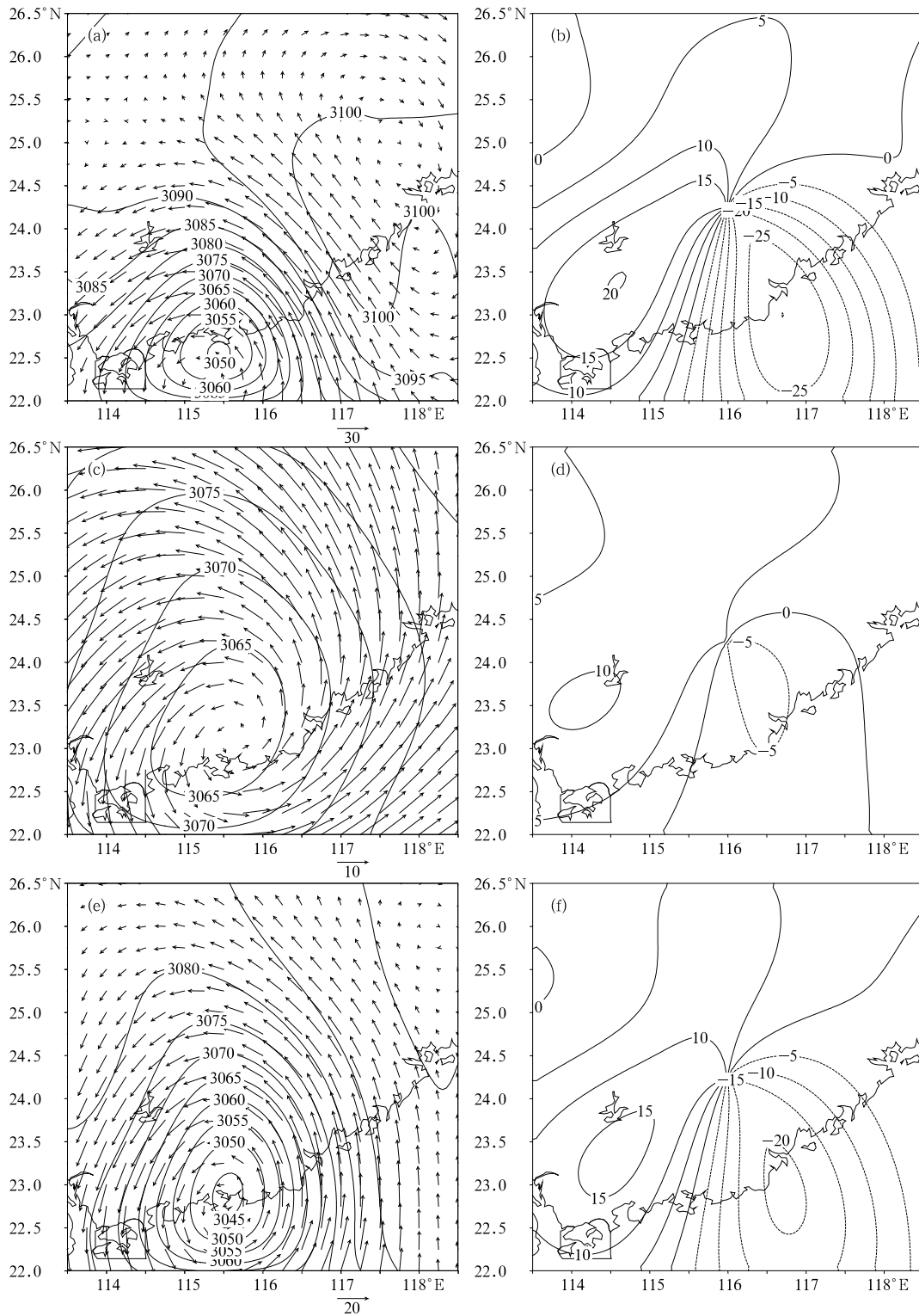


Fig.10. The analyzed wind fields (m s^{-1}) with radar data in Meizhou, Guangdong Province. (a) Radial velocity assimilated, (b) the radial component corresponding to that in Fig.7a, (c) “apparent velocity” assimilated, (d) the radial component corresponding to that in Fig.7c, (e) both radial velocity and “apparent velocity” assimilated, and (f) the radial component corresponding to that in Fig.7e.

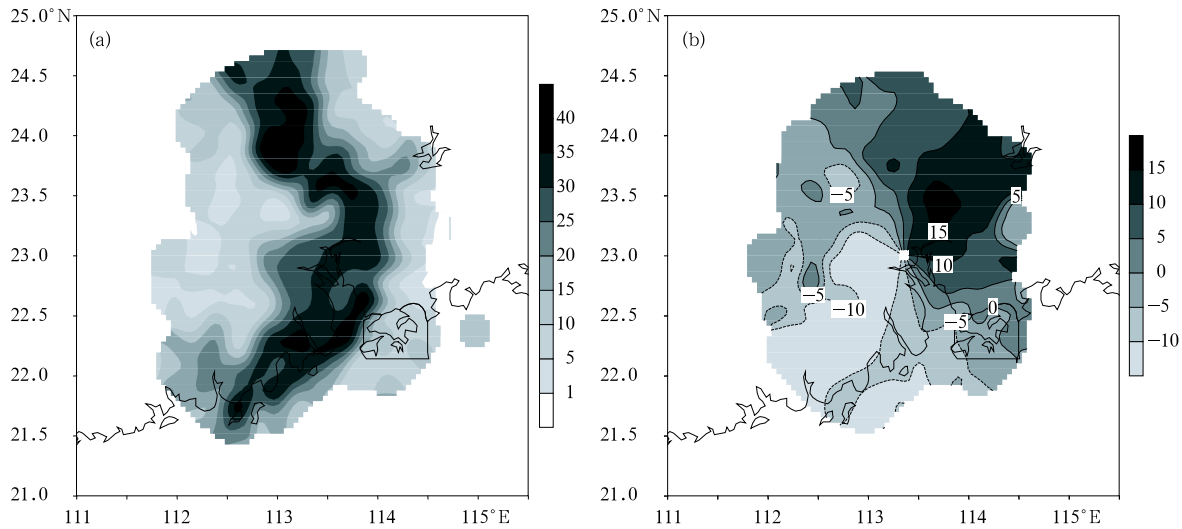


Fig.11. Radar data in Guangzhou city, Guangdong Province at the height of 3 km (03061012UTC). (a) Radar echo intensity (dBz), and (b) radial velocity (m s^{-1}).

Figure 12 gives the wind field acquired with the variational and assimilation scheme using radar data from Guangzhou city, Guangdong Province (at the height of 3km). Figures 12a and 12b give the wind field and divergence field of assimilated radial wind velocity (in contours, the same below) and the radial component in relation to the radar. Figures 12c and 12d give the wind field and divergence field of assimilated “apparent wind velocity” and the radial component in relation to the radar. Figures 12e and 12f give the wind field and divergence field of assimilated radial wind velocity and “apparent wind velocity” and the radial component in relation to the radar. Figures 12g and 12h give the wind field and divergence field analyzed with radiosounding data. Although the determined radial wind velocity agrees with that measured by radar, the southwesterly is the dominant wind over the analyzed area and realistic wind field is obtained, the location of convergence center does not correspond well with the area of intense radar echo. If only the “apparent wind velocity” is assimilated, largely accurate wind fields can also be determined but with much smaller radial component in the southwest sector and poor corresponding relationship between the convergence center and the area of intense echo. Only with joint assimilation of the radial wind velocity and “apparent wind velocity” can we have the most realistic

wind field—not only the radial component of wind field is close to that measured by radar but the divergence center corresponds well with the area of intense radar echoes. In other words, the result is the best when the radial wind velocity of radar and information about the “apparent wind velocity” are jointly assimilated and its mesoscale convergence matches well with the area of intense radar echoes. Meantime, one must note that the wind field analyzed with radiosounding data (Figs.12g and 12h) cannot have mesoscale convergence that match the area of intense radar echoes.

Figure 13 gives the cross section at 113.35°E (through the radar). Figure 13a gives the vertical velocity determined by jointly assimilating the radial and “apparent” wind velocity and Fig.13b gives the intensity of corresponding radar echoes. The figures show that two areas of ascending motion in the determined wind field are corresponding to intense radar echoes, indicating that the wind field acquired with the variational and assimilation scheme reflects well an observed convection and mesoscale wind field structure.

5. Conclusions

The following conclusions can be drawn from the analyses above:

- (1) The “apparent wind velocity” proposed in this

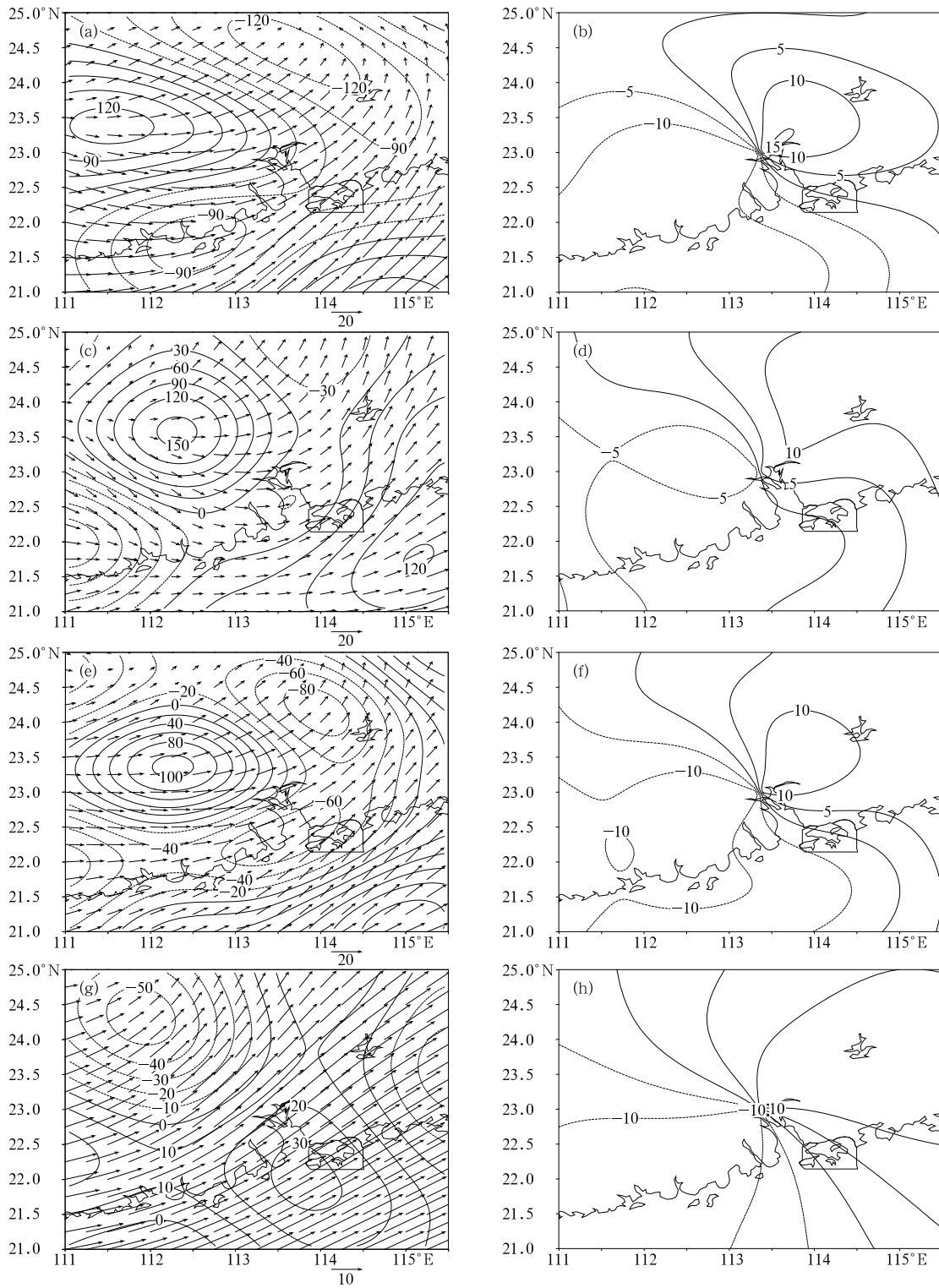


Fig.12. The analyzed wind vector (m s^{-1}) and divergence (10^{-6}s^{-1}) with radar data in Guangzhou city, Guangdong Province. (a) Radial velocity assimilated, (b) the radial component corresponding to that in Fig.7a, (c) “apparent velocity” assimilated, (d) the radial component corresponding to that in Fig.7c, (e) both radial velocity and “apparent velocity” assimilated, (f) the radial component corresponding to that in Fig.7e, (g) radiosounding data assimilated, and (h) the radial component corresponding to that in Fig.7g.

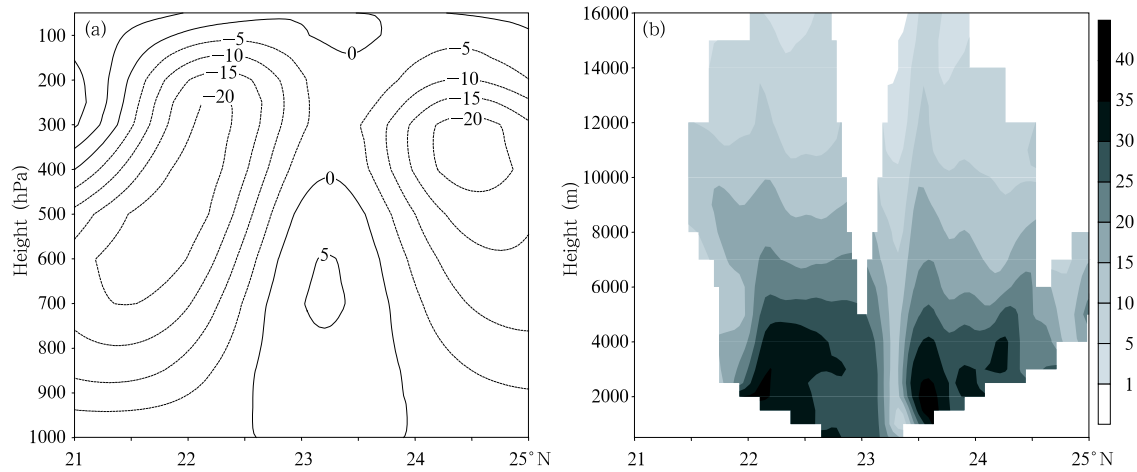


Fig.13. The vertical cross section along 113.35°E (passing through the radar). (a) Vertical velocity ($10^{-3} \text{ hPa s}^{-1}$), and (b) radar echo intensity (dBz).

work is very useful in acquiring the atmospheric wind field.

(2) By using either the radar radial wind velocity or “apparent wind velocity”, the wind field increment obtained with the assimilation analysis will have an advantageous transformation vector in the observations.

(3) Assimilating the radial wind velocity or “apparent wind velocity” only may not obtain realistic wind fields because of the presence of uncertainty. Joint assimilation of the radial wind velocity and “apparent wind velocity” can greatly improve the result.

(4) As shown in the case experiments, the proposed scheme in which radar-measured wind field measurements are directly used in the analysis of mesoscale systems taking place in the vortex and straight basic flow can achieve satisfying results.

(5) The proposed scheme is able to be run operationally and can be combined naturally and directly with other types of observations. It makes it useful in the generation of initial values of NWP. The scheme is also applicable under the existing data condition of the new-generation Doppler weather radars in China.

REFERENCES

- Browning, K. A., and R. Wexler, 1968: The determination of kinematic properties of a wind field using Doppler radar. *J. Appl. Meteor.*, **7**, 105-113.
- Gu Jianfeng, Xue Jishan, and Yan Hong, 2004: A summarization of the four-dimensional variational Doppler radar analysis system. *Journal of Tropical Meteorology*, **20**(1), 1-12. (in Chinese)
- Jiang Haiyan and Ge Runsheng, 1997: A new retrieval technique for single-Doppler radar. *Quarterly J. Applied Meteorology*, **8**, 219-223. (in Chinese)
- Koscielny, A. J, R. J. Doviak, and R. Rabin, 1982: Statistical considerations in the estimation of divergence from single-Doppler radar and application to prestorm boundary-layer observations. *J. Appl. Meteor.*, **21**, 197-210.
- Lang Xuxing, Wei Ming, Dang Renqing et al., 2001: A new method of retrieving wind field using single Doppler radar. *Scientific Meteorology Sinica*, **21**, 417-424. (in Chinese)
- Laroche, S., and I. Zawadzki, 1994: A variational analysis method for retrieval of three-dimensional wind field from single-Doppler radar data. *J. Atmos. Sci.*, **51**, 2664-2684.
- Lhermitte, R. M., and D. Atlas, 1961: Precipitation motion by pulse Doppler radar. Preprints, Ninth Weather Radar Conf, Kansas City, MO, Amer. Meteor. Soc., 218-223.
- Liu Xiaoyang and Liu Guifu, 2000: Difference method for retrieving wind field from single Doppler radar. *Journal of Nanjing Institute of Meteorology*, **23**(4), 549-554. (in Chinese)
- Ma Cuiping, Zhang Peichang, Kuang Xiaoyan et al., 2000: Method of inverting mesocyclone circumfluence field with a single Doppler radar. *Journal of Nanjing Institute of Meteorology*, **23**(4), 579-585. (in Chinese)

- Qiu C. J., and Xu Q., 1992: A simple adjoint method of wind analysis for single-Doppler data. *J. Atmos. Oceanic Technol.*, **9**, 588-598.
- Qiu Chongjian and Xu Qin, 1996: An improvement on the simple conjugate method for retrieving the wind fields from single-Doppler data. *Quarterly J. of Applied Meteorology*, **7**, 421-430. (in Chinese)
- Qiu Chongjian, Yu Jinxiang, and Xu Qin, 2000: Use of Doppler-radar data in improving short-term prediction of mesoscale weather. *Acta Meteorologica Sinica*, **58**(2), 244-249. (in Chinese)
- Scialom, G., and Lemaitre Y., 1990: A new analysis for the retrieval of three-dimensional mesoscale wind fields from multiple Doppler radar. *J. Atmos. Oceanic Technol.*, **7**, 640-665.
- Shapiro, A., S. Ellis, and J. Shaw, 1995: Single-Doppler velocity retrievals with Phoenix data: Clear air and microburst wind retrievals in the planetary boundary layer. *J. Atmos. Sci.* **52**, 1265-1287.
- Smythe, G. R., and D. S. Zrnic, 1983: Correlation analysis of Doppler radar data and retrieval of the horizontal wind. *J. Climate and Appl. Meteor.*, **22**, 297-311.
- Sun J. D., Flicker D., and Lilly, 1991: Recovery of three-dimensional wind and temperature fields from simulated single-Doppler radar data. *J. Atmos. Sci.*, **48**, 876-890.
- Sun J., 1994: Fitting a Cartesian prediction model to radial velocity data from single-Doppler rada. *J. Atmos. Oceanic Technol.*, **11**, 200-204.
- Sun J., and N. A. Crook 1994: Wind and thermodynamic retrieval from single-Doppler measurements of a gust front observed during Phoenix II. *Mon. Wea. Rev.*, **122**, 1075-1091.
- Sun J., and N. A. Crook, 1997: Dynamical and microphysical retrieval from Doppler radar observations using a cloud model and its adjoint. Part I: Model development and simulated data experiments. *J. Atmos. Sci.*, **54**, 1642-1661.
- Sun J., and N. A. Crook, 2001: Real-time low-level wind and temperature analysis using single WSR-88D data. *Wea. Forecasting*, **16**, 117-132.
- Tao Zuyu, 1992: The VAP method to retrieve the wind vector field based on single-Doppler velocity field. *Acta Meteorologica Sinica*, **50**(1), 81-90. (in Chinese)
- Tuttle, J. D., and G. B. Foote, 1990: Determination of the boundary layer airflow from a single Doppler Radar. *J. Atmos. Ocean. Tech.*, **7**, 218-232.
- Tuttle, J., and R. Gall, 1999: A single-radar technique for estimating the winds in tropical cyclones. *Bull. Amer. Meteor. Soc.*, **80**(4), 653-667.
- Waldteufel, P., and H. Corbin, 1979: On the analysis of single-Doppler radar data. *J. Appl. Meteor.*, **18**, 532-542.
- Wu B., J. Verlinde, and Sun J., 2000: Dynamical and microphysical retrievals from Doppler radar observations of a deep convective cloud. *J. Atmos. Sci.*, **57**, 262-283.
- Xu Q., Qiu C. J., and Yu J. X., 1994a: Adjoint-method retrievals of low-altitude wind fields from single-Doppler reflectivity measured during Phoenix II. *J. Atmos. Oceanic Technol.*, **11**, 275-288.
- Xu Q., Qiu C. J., and Yu J. X., 1994b: Adjoint-method retrievals of low-altitude wind fields from single-Doppler wind data. *J. Atmos. Oceanic Technol.*, **11**, 579-585.
- Xu Q., and Qiu C. J., 1995: Adjoint-method retrievals of low-altitude wind fields from single-Doppler reflectivity and radial-wind data. *J. Atmos. Oceanic Technol.*, **12**, 1111-1119.
- Zhang Hua, Xue Jishan, Zhuang Shiyu et al., 2004: Ideal experiments of GRAPES three-dimensional variational data assimilation system. *Acta Meteorologica Sinica*, **62**(1), 31-41. (in Chinese)